SIMPLE, ONCE-OFF MAPPING OF VARIOUS, RECURRENT IMMUNOSTAINING PATTERNS OF PROLIFERATING CELL NUCLEAR ANTIGEN IN SPERMATOGONIA AT THE IMMATURE POLE OF THE TESTIS OF ADULT WILD-CAUGHT BLUE SHARK, *PRIONACE GLAUCA*: CORRELATIONS WITH CHANGES IN TESTICULAR STATUS

Leon Mendel McClusky

Department of Health & Care, Faculty of Health Sciences, UiT The Arctic University of Norway, Campus Narvik, Norway

Corresponding author:

Leon M. McClusky, PhD

Tel: +4776966239

Email: leon.mcclusky@uit.no

Running header: PCNA immunoexpression in immature elasmobranch spermatogonia

Keywords: PCNA immunohistochemistry, stem cell niche, A-spermatogonia, B-spermatogonia, spermatocyst

ABSTRACT

This study was a single time-point mapping of various immunostaining patterns revealed with the Proliferating Cell Nuclear Antigen (PCNA) PC10 antibody in spermatogonia at the immature pole of the testis of the Blue shark (*Prionace glauca*). Scattered in the stroma of the germinal ridge that demarcates the immature pole's outer boundary were nests of variously immunoreactive A-spermatogonia, each flanked by a fusiform cell. Spermatocysts were assembled from niche-derived stromal cells, displaced A-progenitors, and their progeny, that showed one of two main immunostaining patterns (i.e. an uneven light brown/globular and homogeneous dark (hod) brown appearance). The testes of wild-caught *Prionace* showed two conditions, namely extensive multinucleate cell death (MNC) near the mitosis-meiosis transition or an early recovery phase from the latter showing vacuolated areas. Both the proportion of cysts with immature B^{hod}-spermatogonia and the frequency of mitotic figures in such cysts in the early recovery testis condition were significantly higher than the comparable parameters in MNC testis condition. Moreover, the post-MNC recovery phase revealed a decrease in the proportion of immature cysts with uneven light brown/globular-like spermatogonia. The protracted spread of a cell cycle signal in an anatomically discrete syncytially connected spermatogonial clone manifests as different PCNA immunoreactivities.

INTRODUCTION

In all vertebrates, the developmental advance of the primitive spermatogonia through to their transformation into fully differentiated spermatozoa (i.e. the process of spermatogenesis) occurs in the context of a physical and intimate relationship with the germinal compartment's only somatic element, namely the Sertoli cell. Studies mainly in the adult mammalian testis revealed that the founders of spermatogenesis (i.e. the undifferentiated spermatogonia that include the spermatogonial stem cells, SSCs) are located on the seminiferous epithelium's basement membrane at the base of the Sertoli cells and at anatomically ill-defined locations, called stem cell niches (Chiarini-Garcia, Raymer, & Russell, 2003; de Rooij, 2009; Oatley & Brinster, 2012). As a permanent member of the seminiferous epithelium, the higher vertebrate Sertoli cell is palpably a versatile cell, since it additionally and simultaneously nurtures four to five successively layered germ cell stages in its adluminal compartment.

One of the Sertoli cell's well-known stem cell niche functions concerns its secretion of glial cell-derived neurotrophic factor (GDNF) that has stimulatory effects on niche cell kinetics in a range of vertebrates, including the mouse (Ishii, Kanatsu-Shinohara, & Shinohara, 2014; Meng et al., 2000), teleost (Panda, Barman, & Mohapatra, 2011) and even an elasmobranch species (Gautier, Bosseboeuf, Auvray, & Sourdaine, 2014). Moreover, Sertoli niche signaling purportedly also has cell cycle phase-related stimuli on the undifferentiated spermatogonia in the niche. For example, mouse SSCs in G1-phase of the cell cycle were more responsive to Sertoli cell niche signaling to compared to those in S-/G2

through to M phase, and they simultaneously also displayed heightened migration to the stem cell niche if they were in G1-phase of the cell cycle (Ishii et al., 2014).

Whether regulation of the niche population may be the exclusive reserve of the Sertoli cells, is not completely understood, especially in the light of a growing body of evidence from the adult testis in a wide range species, including the zebrafish (Nóbrega et al., 2010), mouse (DeFalco et al., 2015; Potter & DeFalco, 2017; Yoshida, Sukeno, & Nabeshima, 2007) and human (Smith et al., 2014) concerning the role of the interstitial compartment in niche cell kinetics. It is known from mammalian ontogeny at least that the structural rearrangement of the all gonadal cell types into testis cords is the result of not only the collaborative actions of many differentiating Sertoli cells, but also of unidentified non-Sertoli cells and mesenchymal immigration (Nel-Themaat et al., 2009). The relevance of mesenchymal (stromal) –epithelial (Sertoli) cell interactions for adult testicular function in mammals has also been hypothesized (Ema & Suda, 2012; Skinner, 1990).

Teasing apart, however, the supportive roles of the intratubular and extratubular somatic elements towards the mammalian niche population while simultaneously maintaining intact the three-dimensional germ – somatic cell configuration is technically challenging. Alternative vistas for these inquiries in vertebrates may be the adult testes of primitive vertebrates that possess an anatomically well-defined, folliculogenic, stromal cell-rich region at one pole of the organ, from which somatic cell precursors and type A spermatogonia originate to eventually become assembled into spermatocysts (spherical follicle-like units comprising a given germ cell clone and its own complement of Sertoli cells). Electron microscopic study of the niche region in adult specimens of the elasmobranchs *Dasyatus*

Americana and *Carcharinus limbatus* revealed that the singly type A spermatogonia in these two species are in direct contact with interstitial cells (Grier, 1992). The basement membrane that ultimately demarcates the germinal and interstitial compartments, and whose establishment is partly Sertoli cell-driven (Tung, Skinner, Fritz, 1984), is not yet formed around these niche spermatogonia despite the occasional Sertoli cell precursor that borders on these type A spermatogonia (Grier, 1992). Thus, in terms of phylogeny, a somatic element other than the Sertoli cell assumes a greater role in the elasmobranch niche region.

The diametric type testis (Pratt, 1988) of the Blue shark (*Prionace glauca*) displays a prominent stroma-rich folliculogenic region, the germinal ridge (GR), that runs the length of the testis in the midline and demarcates the outer periphery of the immature pole (McClusky, 2013). The latter study on wild-caught summer-aggregating males reported that the GR was ostensibly unscathed by the presence of two seemingly very different histological perturbations among mainly mature B-spermatogonial spermatocysts. The one type of testicular condition, termed the vacuolated appearance, referred to cell-free spaces in the cysts due to Sertoli cell phagocytic clearing up of multinucleate cell (MNC) corpses in these cysts that formed during an earlier wave of cell death (the MNC condition) that swept across the testicular diameter (McClusky, 2013).

It is of great interest therefore to revisit some aspects of prespermatogenesis and the commitment to spermatogenesis proper in the immature pole as they pertain to these two spontaneously occurring perturbations in normal spermatogenesis of free-ranging *Prionace glauca*. The overall objective is to assess the immunohistochemical staining patterns of the conserved cell cycle marker, Proliferating Cell Nuclear Antigen (PCNA), seen in immature

spermatogonia in paraffin sections of field-sampled testes within the context of the existing body of knowledge of the spatiotemporal advance of topographically arranged cysts in the diametric elasmobranch testis such as that of *P. glauca* (McClusky, 2012, 2013; Simpson & Wardle, 1967). PCNA is initially synthesized in early G1-phase of the cell cycle in proliferating cells, and acts as an auxiliary protein to DNA polymerase-delta during S-phase (Bravo, Frank, Blundell, & Macdonald-Bravo, 1987; Prelich et al., 1987). This, together with its peak immunoexpression in S-phase and the purported 20-hour half-life of endogenous PCNA in cycling cells (Bravo & Macdonald-Bravo, 1987), renders the immunodetection of this cell cycle marker suitable for study in all optimally formalin-fixed paraffin-embedded tissues (Dietrich, 1993; Hall & Woods, 1990). To date, the qualitative and quantitative PCNA immunohistochemical analyses of spermatogonial generations of higher vertebrates (Chapman & Wolgemuth, 1994; Saunders, 2003; Schlatt & Weinbauer, 1994; Wrobel, Bickel, & Kujat, 1996) and lower vertebrates (Loppion, Crespel, Martinez, Auvray, & Sourdaine, 2008; McClusky, 2005; Yazawa, Yamamoto, Nakayama, Hamada, & Abé, 2000) have only distinguished between PCNA-positive and PCNA-negative cells. Other variations of PCNA immunostaining were either not reported or presumably not discernable. It is conversely hypothesized with this study in the Blue shark that the protracted rates of cellular development in this cold-blooded vertebrate would in all likelihood manifest as differential immunohistochemical patterns among the members of the syncytial germ cell clone (i.e. the cyst), particularly so if one or several clone members are patently engaged in mitotic division.

One specific aim of this retrospective study of archival cross-sections is to perform a single time-point (i.e. at time of dissection) spatial mapping of the main PCNA immunostaining patterns observed in (1) niche-located A-spermatogonia, (2) committed A-spermatogonia that are gradually displaced towards the area where cysts are assembled, and

(3) newly cyst-enclosed B-spermatogonia. A second aim is to explore quantitatively for correlations between the major PCNA immunostaining patterns displayed by the immature cysts' B-spermatogonia and the frequency of mitotic figures in the same cysts, all expressed as a function of the two testicular conditions observed in these summer-aggregating male *P. glauca* specimens.

MATERIALS AND METHODS

Animals

Prionace glauca is a pelagic shark species with a circumglobal distribution in temperate and tropical waters. The two sexes congregate on the continental shelf off southern New England (USA) during the summer months for purposes of mating (Pratt, 1979) after which they depart in October towards warmer waters. Considering the status of *P. glauca* as a near-threatened species, it is important that opportunities that provide access to tissues are fully exploited as a year round investigation into the reproductive biology of this species is hampered by a lack of specimens. This study is based on testes dissected from 11 adult males selected from a larger sample (n=19; 67.3 – 120 kg; 213 – 262 cm fork-length) as these contained the testicular regions of interest for this study. These adult specimens (many with their hearts still beating) were landed together with other apex predators by recreational fishermen participating in sports-fishing tournaments over the summer months at Montauk (New York) and Martha's Vineyard (Massachusetts) in June-July as reported previously (McClusky, 2018). All subsequent animal handling and dissection procedures were

performed under the auspices and ethical approval of the National Oceanic and Atmospheric Administration Fisheries Service, Narragansett (RI) and its attending fisheries scientists who catalogued all landed species as part of their Apex Predators Program.

Tissue preparation and immunohistochemistry

At least two to three cross-sections (3 – 5 mm) were cut midway along the length of both testes, fixed immediately in 10% buffered elasmobranch formalin (Prieur, Fenstermacher, & Guarino, 1976) for not more than 48 hours after which tissues were stored in 70% ethanol until further processing. Tissues were embedded in paraffin wax and processed for routine histology and immunohistochemistry. Paraffin sections of 4-5 μm thickness were generated and collected on silicane-coated glass slides, dried for 30 min at 60 °C, deparaffinized and rehydrated stepwise through a graded ethanol series prior to routine histological examination with Gills II hematoxylin and eosin staining and immunohistochemistry.

PCNA immunohistochemistry

The immunohistochemistry protocol followed was that as previously optimized for use on elasmobranch tissues (Borucinska, Schmidt, Tolisano, & Woodward, 2008; McClusky, 2005). Briefly, endogenous peroxidase activity was quenched by treating rehydrated sections in darkness with 3% hydrogen peroxide. Following a rinse in distilled water, sections were subjected to an antigen retrieval procedure, which entailed incubation for 10 min in "Retrieve-all" pH 8.0 (Signet Laboratories, Dedham, MA, USA) in a steamer bath, followed by 10 min 'cool down' at RT. After two washes in diluted Cadenza buffer wash (Thermo

Electron Corp., Waltham, MA, USA), which was also used in all subsequent washes, sections were then incubated with Omnitags protein blocking solution (Thermo Electron Corp., Waltham, MA, USA) for 5-10 min at RT to reduce non-specific binding, and then overnight at RT with anti-PCNA PC10 (a mouse monoclonal antibody derived against a recombinant mouse PCNA consisting of amino acids 112-121; Calbiochem, San Diego, CA, USA) at final concentration 0.001 $\mu g\ \mu L^{-1}$.

After three buffer washes, sections were incubated at 1:40 dilution in biotinylated anti-mouse secondary antibody (Thermo Electron Corp., Waltham, MA, USA) for 30 min at RT. Following three buffer washes, sections were incubated with the Vectastain streptavidin-peroxidase complex (Vector Laboratories, Burlingame, CA, USA) for a further 20 min at RT. The antigen was finally detected by treating the sections with Vector Nova Red substrate kit (Vector Laboratories, Burlingame, CA, USA) for 10 min, counterstained with Shandon Gill 2 hematoxylin (Thermo Electron Corp., Waltham, MA, USA), dehydrated, cleared and mounted with Permount (Fisher, Fairlawn, NJ, USA). The sectioning of each paraffin block always included a section for negative control staining, which entailed incubating such a section with optimally diluted mouse isotype antibody (Thermo Electron Corp., Waltham, MA, USA). Human tonsil sections were additionally processed as positive controls.

Microscopy and analysis

Sections were viewed, analysed and the regions of interest photographed with a Leica DMLS bright field microscope fitted with a Visicam 5.0 digital camera (VWR, Belgium). Analyses focused on the immature pole of testis, namely the stem cell region which is the thin, but prominent white germinal ridge (GR) running in the midventral surface and continuous with

the tough fibrous testicular capsule, and the immediately adjacent region, namely the germinal zone (GZ) where cysts are assembled and spermatogonial differentiation commences. In all elasmobranchs, the latter manifests histologically as the gradual rearrangement (here termed the *non-patterned* cyst stage) of the cyst's cellular contents with respect to the Sertoli cell nuclei that ultimately and exclusively assume a perilumenar position (here termed the *patterned* cyst stage).

Analyses of the types of PCNA immunoreactivities observed in the population of GR-located A-spermatogonia were quantified as the proportions of each type of immunoreactive A-spermatogonium calculated from the total absolute number of A-spermatogonia counted per testicular section, expressed as a function of the type of closest aligned somatic cell. Absolute counts were made of the A-spermatogonia as their occurrence in the GR appeared to be sporadic, and their numbers highly variable to the extent that the GRs of some testicular sections showed no spermatogonia. Quantitative analyses of all immature spermatogonial cyst stages was based on the earlier classification of each testis sample as belonging to either the multinucleate cell-type or vacuolated type of degeneration, as previously reported (McClusky, 2013). Briefly, a given testicular cross-section of an animal was designated as either the multinucleate cell-type or vacuolated type of degeneration based on whether a cyst revealed a minimum of either three clusters of multinucleate giant cells or three large vacuolated spaces). For quantification of the proportions of non-patterned cysts whose spermatogonia display a given type of PCNA immunostaining architecture expressed as a function of testicular condition, all cysts that intersected or were contiguous to three lines (in the eyepiece) that radiated from the fibrous GR were counted, classified by stage and its PCNA immunostaining pattern. For quantification of the mitotic index per immature spermatogonial cyst, all nonpatterned and earliest patterned cysts that intersected or were contiguous to four lines (for

purposes of obtaining sufficient numbers of mitotic figures) that radiated from the GR, were counted, classified according to the observed PCNA immunostaining architecture and their total number of mitotic figures noted.

Statistical analysis

Quantitative data were analysed by one-way analysis of variance (ANOVA) using InStat version 2.03 (GraphPad Software, San Diego, CA). See individual figure legends for detailed descriptions.

RESULTS

Fig.1A depicts schematically the organization of the immature pole of the testis whose outer boundary is defined by the germinal ridge (GR). The GR is the folliculogenic region as it houses the type A spermatogonia, which are found in island-like clusters, here termed the germinal nests. The first indication of the proper formation of testicular parenchyma is in the subsequent testicular region, namely the germinal zone (GZ) in which the first cysts are noted (Fig. 1A). The latter development is the morphological manifestation that the process of spermatogonial differentiation has commenced. The term “germinal nest” was coined to define a distinctive histoarchitecture only seen in the GR, namely the clustering of large spherical spermatogonia during which each spermatogonium is flanked by a fusiform somatic cell in a crescent-like fashion (Fig. 1B). Scatterings of single or small groups of A-spermatogonia simultaneously revealed the occurrence of another somatic cell type in the GR, namely large stromal cells that usually accompanied isolated spermatogonia (Fig. 1B). The

latter somatic cells were prevalent in the GZ and were observed arranged in rows adjacent to the now dispersed-looking A-spermatogonia (Fig. 1B).

The type A spermatogonia in the GR comprised a heterogeneous population of germ cells as revealed by PCNA immunohistochemistry (Fig. 2). The crisp nuclear immunostaining accentuated the main differences in the architectural patterns displayed by the nucleus (speckled and homogeneous) and the magnitude of the cytoplasmic compartment, all of which assisted in the discrimination between spermatogonia with PCNA-negative speckled (*neg*), light speckled brown (*lsp*), dark speckled brown (*dsp*) and intense homogeneous dark brown (*hod*) nuclei, the latter also usually revealing a single blue-grey nucleolus (Fig. 2A). Single and smaller groups of A-spermatogonia, typically accompanied by aggregations of large oblong stromal cells, were also scattered throughout the GR (Fig. 2B). The latter somatic cells were conspicuous by their presence among dispersed-looking A^{hod}-spermatogonia in the GR stroma (Fig. 2C). Unlike with the A-spermatogonia with speckled nuclei, variations in the quality of the PCNA immunostaining of A^{hod}-spermatogonia were dramatic, such as during diminishing PCNA immunoreactivity (Fig. 2C) or when these A-spermatogonia were observed as part of chains of other seemingly unrelated immunonegative cells (Fig. 2D). Despite the latter's immunonegative status, the still discernible identically sized nucleolus and the faint remnants of PCNA immunostaining all testified of an affiliation between these immunonegative cells and A^{hod}-spermatogonia (Fig. 2D). The intense brown immunostaining as seen in, for example A^{hod}-spermatogonia, was quite distinct from the sporadic anomalous PCNA immunolabeling of a lone shrunken, patently dying A-spermatogonium (Fig. 2E), phenomena that ultimately resolved as pyknotic death that is well discerned from other stages of cell death (Fig. 2F).

The above qualitative observations of the germline in the GR seemed to indicate an association between the type of PCNA immunostained A- spermatogonium and the type of the closest aligned somatic cell (see Fig. 2C). To explore this correlation quantitatively, the proportions of each of the three categories of PCNA-immunostaining displayed by A-spermatogonia were expressed as a function of somatic cell type (Fig. 3). Overall, differences in the proportions of each type of PCNA-immunopositive A-spermatogonium associated with a given somatic cell were highly significant ($P < 0.0001$), although the A^{dsp}-spermatogonia displayed no preferential association with either somatic cell type. A significant ($P<0.05$) four-fold higher proportion of A^{lsp}-spermatogonia was solely associated with fusiform cells compared to the proportion that was exclusively surrounded by irregular shaped/large oblong cells. Conversely, a significant ($P < 0.001$) three-fold higher proportion of A^{hod}-spermatogonia (related blue and partially immunostained cells) was solely associated with irregular shaped/large oblong cells compared to the proportion of these spermatogonia still encircled by the fusiform cell.

Figs. 4 and 5 show that the above immunostaining patterns of the A-spermatogonia were likewise observed in the cysts and groups of stromal-cell enclosed A-progenitors that presaged cyst assembly in the GZ, phenomena that largely explained the two different histoarchitectures seen in the GZ. Commitment to spermatogenesis proper of a group of synchronously advancing A^{hod}-progenitors manifested as disparate immunostaining patterns such as a marked lightening in brown immunostaining, developments that were related to entry into mitosis (Fig. 4A). The gradual rearrangement of these immature spermatogonia with respect to their associated stromal cells, such as to signal the assembly of the first cysts, were coincident with a broader spectrum of these diffuse immunostaining patterns (Fig. 4B). The significance of the latter was evident during subsequent cyst growth during which some

members of the syncytially connected spermatogonial clone were already in M-phase simultaneously as other clone members had a diffused, uneven brown appearance or revealed an increasing number of globular translucent areas against the dark brown background (Fig. 4C). No signs of mitosis were, however, noted in those B^{hod}-spermatogonial clones that instead revealed diminishing PCNA immunostaining with resultant basophilia (Fig. 4D).

In contrast, the GZ that nearly exclusively featured dark speckled brown progenitors and early B-spermatogonia in the first appearing cysts revealed a markedly different histoarchitecture (Fig. 5). PCNA immunohistochemistry readily discriminated between strongly immunoreactive A^{dsp}- progenitors and the inimitable A^{hod}-progenitors in this histoarchitecturally distinct GZ as the former's underlying inherent speckled nuclear architecture was palpably still evident despite their strong PCNA immunoreactivity.

The significance of these two types of histoarchitectures of the GZ was unclear. The gradual unveiling of globular-looking translucent areas in the B^{hod}-spermatogonia led to a change that was reminiscent of that of the nuclear architectural pattern of the dark speckled brown spermatogonia. It was then determined to screen the rest of the immature pole for the development of these globular-looking translucent areas in all subsequent cyst stages that housed B^{hod}-spermatogonia or closely related spermatogonia.

The rare fortuitous sight of an early patterned cyst that simultaneously housed B^{hod}-spermatogonia and B-spermatogonia with an uneven light brown, globular-like appearance demanded further scrutiny (Fig. 6). Closer examination revealed that the increased presence of small globular-like translucent areas in the B^{hod}-spermatogonia ultimately resulted in the

uneven light brown, globular-like appearance (Fig. 6). The latter change accounted, in part, for appearance of multiple rows of cysts with uneven light brown, globular-like spermatogonia. Further scrutiny of the latter spermatogonia revealed that the uneven light brown, globular-like appearance additionally referred to the step-wise, conspicuous thickening and separation of chromatin into distinct strands that typified prophase (Fig. 6). Thus, the appearance of cysts consisting entirely of uneven lighter brown/globular-like spermatogonia possibly represented a pronounced protracted or a delay in their progression through to M-phase.

An earlier study of the same specimens reported two histological perturbations of cell death among mainly the mature B-spermatogonial cysts, phenomena that led to the grouping of the sampled testes into those with the multinucleate cell death (MNC) or vacuolated testis conditions (McClusky, 2013). Although useful for systematic analyses, these distinctions were robust as they essentially referred to two phases of the same protracted cell death phenomenon. The vacuolated areas appeared in the cysts due to Sertoli cell phagocytic clearing up of the dead MNC corpses in these cysts simultaneously as a recovery phase commenced from the earlier wave of cell death. The initial robust quantitative analyses of the PCNA immunoreactivities of the spermatogonia at the immature pole of the same samples were also inconclusive.

Given therefore what appears to be alternate junctures in the advance of immature B-spermatogonia towards mitosis (Fig. 6), it was therefore determined to quantify these major staining patterns in immature spermatogonia in terms of the frequency of observed mitotic figures per cyst (i.e. mitotic index), expressed as a function of the above two testicular

conditions (Fig. 7). Overall, the calculated differences in the mitotic index with any given nuclear architectural pattern were extremely significant (P = 0.0007) in both testicular conditions (Fig. 7). As expected, the total mitotic index in cysts with uneven light brown/globular-like spermatogonia for both testis conditions combined was more than two-fold higher than that in cysts with homogeneous dark brown stained spermatogonia. Concerning the group of testes with the vacuolated appearance, there was no significant difference between the mitotic index in cysts that housed uneven lighter brown/ globular-like spermatogonia and that in cysts that housed homogeneous dark brown B-spermatogonia. However, the mitotic index in the latter cysts (with homogeneous dark brown B-spermatogonia) was significantly (P < 0.01) more than 3-fold higher in the vacuolated testis condition than the corresponding index in the same cyst group in the MNC testis condition. In the testes grouped as the multinucleate cell (MNC) death testis condition, the mitotic index in cysts containing uneven lighter brown/ globular-like spermatogonia was significantly (P < 0.01) and more than 4-fold greater than that in cysts with homogeneous dark brown B-spermatogonia.

As the above data were calculated as the frequency of the mitotic figures per cyst, it was further determined to corroborate these findings in terms of proportions of immature spermatogonial cysts whose spermatogonia displayed either one of the two major immunostaining patterns observed, expressed as a function of testis condition (Fig. 8). Overall, the calculated differences in the proportions of nonpatterned cysts with any given architectural pattern were extremely significant (P <0.0001) in both testicular conditions. As above, the total proportion of non-patterned cysts with uneven light brown/globular-like spermatogonia for both testis conditions combined was 1.9 fold higher than that of cysts with homogeneous dark brown stained spermatogonia. However, the proportion of cysts in the

vacuolated testis condition with uneven light brown/globular-like B-spermatogonia was significantly ($P < 0.05$) 1.7-fold less than the comparable proportion of cysts in the MNC testis condition. By comparison, the proportion of cysts in the vacuolated testis condition with homogeneous dark brown B-spermatogonia was significantly ($P < 0.01$) greater 3-fold than the comparable proportion of cysts in the testes with the MNC condition.

DISCUSSION

Available data from a wide range of species regarding the cellular composition of the stem cell niche are unanimous that the occurrence of pale and dark A-spermatogonia, typically seen in the higher primate testis (Clermont, 1966; Oatley & Brinster, 2012; Plant, 2010), is the exception rather than the rule among the vertebrates. This report though of pale and dark niche A-spermatogonia in an elasmobranch, together with similar findings in the frog (Haczkiewicz, Rozenblut-Kościsty, & Ogielska, 2017; Rastogi, DiMeglio, DiMatteo, Minucci, & Iela, 1985) not only confirms the existence of the dark A-spermatogonia at lower levels of phylogeny, but also adds to the debate about the plasticity of the functional tissue architecture of the vertebrate stem cell niche.

The findings reported here for a pelagic elasmobranch of large nests of pale and dark A-spermatogonia in a conspicuous niche region are novel. It is postulated that these probably indicate species-specific differences among elasmobranchs and/or hitherto poorly understood aspects of the site of origin of the cysts that arise in the chondrichthyan folliculogenic region. The latter is nearly always neglected in fisheries research type of investigations into male reproduction owing to the focus on sperm production. Moreover, the full extent of the GR is

rarely seen in testicular cross-sections in the latter investigations since it is either macroscopically unremarkable, ill defined, and/or not properly retained during transverse sectioning of the fresh testis. The lack of appropriate precautionary measures during the latter disproportionately affects the retention post-fixation of the tough testis capsule that is continuous with the GR (compare (Bosseboeuf, Gautier, Auvray, Mazan, & Sourdaine, 2014; Gautier et al., 2014; McClusky, 2005; Parsons & Grier, 1992).

In contrast though the few scattered PCNA immunohistochemical investigations of the elasmobranch testis, namely that on the seasonal spiny dogfish (McClusky, 2005) and on the non-seasonal lesser-spotted dogfish (Loppion et al., 2008) were conducted as part of basic research inquiry, and even here the GR was under-reported for reasons mentioned above. As showed in this study of the GR in *P. glauca* and that of the seasonal spiny dogfish (McClusky, 2005), any cytoarchitectural differences among spermatogonia in this prodigiously active testicular region are likely to be accentuated by PCNA immunohistochemistry, due to the completely different time-line (e.g. protracted and episodic) of essential ongoing self-renewal decisions and commitment to spermatogenesis proper in these two migratory species compared to that in the continuously breeding laboratory rodent (Hilscher, Hilscher, & Maurer, 1966). These notions are plausible considering that even the undifferentiated spermatogonia of the adult rat have considerably long S- and G2-phases (Huckins, 1971b). Differences in the functional histoarchitecture of the stem cell niche in the lesser-spotted dogfish and the Blue shark as reported here, concerns the size dimensions of the niche, its constituent somatic elements, and how the latter relate to both the PCNA-positive and PCNA-negative A-spermatogonia. The available photographic evidence of the niche population in the lesser-spotted dogfish suggest that the niche comprises exclusively of the speckled brown A-spermatogonia, which may render any further direct

comparisons with the present study tenuous. For example, this single time-point "window" into ongoing cell kinetics at the immature pole of *P. glauca* was carried out on recreationally fished and field-sampled, formalin-fixed testes of wild-caught, reproductively active males. By comparison, the study of Loppion et al. (2008) involved acetic acid-based fixation of laboratory-sampled testes from specimens of a smaller-sized non-seasonal dogfish species that were acclimatized for two weeks in seawater tanks after capture in their littoral zone habitat. Lastly, it is worth noting that Loppion et al. (2008) employed the much less sensitive DAB as reporter enzyme in the final step of their immunohistochemical protocol, which differed from this study in *P. glauca* that used the more sensitive Vector Nova Red as reporter. It is therefore proposed that the above species differences in PCNA immunoreactivities of the niche A-spermatogonia may instead relate to the dissimilar habitats and reproductive ecologies of these two species. Fig. 9 summarizes the putative functional interrelationships of all spermatogonia, from the stem cell region (GR) and downstream into the adjacent GZ and early premeiotic region of the testis of *P. glauca*.

In the first ever PCNA immunohistochemical study of the elasmobranch testis (i.e. spiny dogfish), the A-spermatogonia observed in the turgid, triangular shaped GR (typically seen in the period of peak spermatogenic activity (spring – summer)) stained intensely dark brown (McClusky, 2005). There was, however, no trace of such A-spermatogonia during the period of spermatogenic inactivity (late fall – winter) when the GR lacked an apex and was almost flap-like in cross-section (McClusky, 2005). These novel findings of the elasmobranch stem cell region were not investigated further.

Given the dearth of knowledge about the founders of elasmobranch spermatogenesis, it may be worth reevaluating the published histology photomicrographs of the niche A-spermatogonia of the bonnethead shark (Parsons & Grier, 1992). The nucleus of one of the three spherical spermatogonia is clearly larger, displays a conspicuous nucleolus against the granular background, all of which are morphological characteristics that seem to match a correspondingly H&E-stained A^{hod} -spermatogonium reported here for the Blue shark (see inset, Fig 2D). The bonnethead shark's pale A-spermatogonium with its speckled nucleus, is nevertheless identical to that seen in most elasmobranch species, including the lesser spotted dogfish (Dobson & Dodd, 1977; Gautier et al., 2014; Loppion et al., 2008), soupfin shark (unpublished observations) and shortfin mako shark (unpublished observations) that was co-landed with the Blue shark in this study.

The synchronized spread of a given intracellular signal in a syncytially connected clone of germ cells is a central tenet of germ cell developmental advance in the vertebrate testis. Since the anatomically discrete elasmobranch germinal clone is sealed off from other clones, the seemingly unrelated differential PCNA immunostaining patterns observed in a single syncytially connected B-spermatogonial clone are meaningful when understood in the context of the protracted rates of cellular development in these poikilotherms, more so if one or several clone members have entered M-phase. An unexpected finding concerns the prevalence of spermatogonia with an uneven light brown, globular-like/diffused immunostained appearance in entire cysts or in one area of the cyst. Scrutiny at high magnification of uneven light brown, globular-like spermatogonia reveal that this classification also referred to the step-wise, conspicuous thickening and separation of chromatin into distinct strands that typified prophase (see Fig. 6). These notions are in broad agreement with several scattered reports concerning G2-phase cells and their PCNA immunoreactivity. G2 nuclei were noted

for the increasing separation of their chromatin into distinct strands, during which the corresponding anti-PCNA staining with in vitro immunofluorescence and immunohistochemistry were described as spotty (Hutchison & Kill, 1989), and diffused and speckled (Foley, Dietrich, Swenberg, & Maronpot, 1991), respectively. By extension then, entire cysts containing only uneven lighter brown/globular-like spermatogonia are posited to represent a pronounced protracted progression through to M-phase or a delay in their developmental advance. Conversely, the presence of only a small subset of uneven lighter brown/globular-like spermatogonia in the cyst together with others who are already in mitotic division suggest late G2/imminent entry into prophase.

The cytoarchitectural differences between strongly immunoreactive A^{dsp}- progenitors and A^{hod}-progenitors remain distinct since the former's underlying inherent speckled nuclear architecture was not masked by even strong PCNA immunoreactivity. It is posited that the differences between these two major types of progenitors may be more real than apparent. Fig. 9 presents a tentative scheme for developmental advance of committed A-spermatogonia from the stem cell region (GR) downwards into the premeiotic region of the testis. Despite the presence, in the GZ, of sometimes both A^{dsp}-progenitors and A^{hod}-progenitors that may even border on each other, the ensuing histoarchitecture of the GZ reflects the commitment to spermatogenesis proper, and subsequent assembly of cysts, of only one of the two major types of progenitors. Thus, the differential PCNA immunostaining patterns observed, within and among the early PrM cysts indicate the predominant cell cycle phase that was spreading through the spermatogonial clone at that the time of sampling. Accordingly, entire cysts with only uneven light brown/globular-like B-spermatogonia (Fig. 9a) possibly represent a pronounced protracted progression or a delay in G2, all which presumably also apply to the developmental advance of A^{dsp}-progenitors from which such cysts develop.

Conversely, B^{hod}-spermatogonia (hypothesized to represent late G1−S -phase) in other developing cysts are postulated to result from the developmental advance of A^{hod}-progenitors (Fig. 9c). The diverse PCNA immunostaining patterns on display in the various syncytially connected members of a single such spermatogonial clone, include several PCNA-negative members in mitotic division, those revealing distinct separate chromatin strands, and others with an uneven light brown/globular-like appearance. Taken together then, all the latter immunomorphologies clearly indicate a *shortened* G2-phase/imminent entry into prophase as other clone members had already progressed through into M-phase (Fig. 9c). By extension, the presence, in the same clone, of two successive cell cycle phases is hypothesized to imply "quicker cycling" through to M-phase. These notions are in agreement with the quantitative analysis of the two major types spermatogonial cysts observed in the two testis conditions. For instance, the large significant increase in the mitotic index of small cysts containing B^{hod}-spermatogonia in the early recovery phase condition (see Fig. 8), together with, in the same testis condition, the significant decrease the proportion of late G2-phase/imminent prophase-spermatogonial clones (i.e. uneven light brown/globular-like) allude to the restoration of the appropriate balance in the proportion of immature spermatogonial clones post-MNC recovery in the testis of *P. glauca*. Interestingly, the early differentiating mammalian spermatogonium is also known to alter the duration of some of its cell cycle phases. Classic cell kinetic experiments in the testis of the continuously reproductively active rodent reported a progressive lengthening of S-phase and concomitant significant shortening of G2-phase during particularly the transition from A_1 to A_3 spermatogonia (Huckins, 1971a). These notions are broadly consistent with the known synchronization of the developmental advance of germ cells within and between spermatogenic stages, as previously noted in primitive

(Betka & Callard, 1998; Piferrer & Callard, 1995) and advanced vertebrates (Blanco-Rodriguez, Martinez-Garcia, & Porras, 2003; Kerr, 1995; Miething, 2010).

In conclusion, these findings of PCNA immunohistochemistry in a highly migratory species like *P. glauca* provide evidence of novel, recurrent immunostaining patterns of the germ line, first noted in the stem cell region. Although further elucidation is required, cross-checking of the gradual waxing and waning PCNA immunoreactivities, and changes in hematoxylin blue staining of syncytially connected spermatogonial clones in a cluster of contiguous cysts utility in generating hypotheses about the putative cell cycle phases, especially so if one or more members of the spermatogonial clone member are already in mitosis.

ACKNOWLEDGMENTS

This study was funded, in part, by a grant from the former Narvik University College, which has since been incorporated as Campus Narvik into the University of Tromsø – The Arctic University of Norway. The author is greatly indebted to Dr. J. Borucinska of the Department of Biology, University of Hartford, and Dr. D Wood of the Department of Pathobiology and Veterinary Sciences, University of Connecticut, CT, USA for supplying the tissues and the PCNA immunohistochemistry work.

REFERENCES

Betka, M., & Callard, G. V. (1998). Negative feedback control of the spermatogenic progression by testicular oestrogen synthesis: insights from the shark testis model.

Acta Pathologica, Microbiologica, et Immunologica Scandinavica, 106(1), 252-257; discussion 257-258.

Blanco-Rodriguez, J., Martinez-Garcia, C., & Porras, A. (2003). Correlation between DNA synthesis in the second, third and fourth generations of spermatogonia and the occurrence of apoptosis in both spermatogonia and spermatocytes. *Reproduction, 126*(5), 661-668.

Borucinska, J. D., Schmidt, B., Tolisano, J., & Woodward, D. (2008). Molecular markers of cancer in cartilaginous fish: immunocytochemical study of PCNA, p-53, myc and ras expression in neoplastic and hyperplastic tissues from free ranging blue sharks, *Prionace glauca* (L.). *Journal of Fish Diseases, 31*(2), 107-115. doi:10.1111/j.1365-2761.2007.00871.x

Bosseboeuf, A., Gautier, A., Auvray, P., Mazan, S., & Sourdaine, P. (2014). Characterization of spermatogonial markers in the mature testis of the dogfish (*Scyliorhinus canicula* L.). *Reproduction, 147*(1), 125-139. doi:10.1530/rep-13-0316

Bravo, R., Frank, R., Blundell, P. A., & Macdonald-Bravo, H. (1987). Cyclin/PCNA is the auxiliary protein of DNA polymerase-δ. *Nature, 326*(6112), 515-517. doi:10.1038/326515a0

Bravo, R., & Macdonald-Bravo, H. (1987). Existence of two populations of cyclin/proliferating cell nuclear antigen during the cell cycle: association with DNA replication sites. *Journal of Cell Biology, 105*(4), 1549-1554.

Chapman, D. L., & Wolgemuth, D. J. (1994). Expression of proliferating cell nuclear antigen in the mouse germ line and surrounding somatic cells suggests both proliferation-dependent and -independent modes of function. *The International Journal of Developmental Biology, 38*(3), 491-497.

Chiarini-Garcia, H., Raymer, A. M., & Russell, L. D. (2003). Non-random distribution of spermatogonia in rats: evidence of niches in the seminiferous tubules. *Reproduction, 126*(5), 669-680.

Clermont, Y. (1966). Renewal of spermatogonia in man. *American Journal of Anatomy, 118*(2), 509-524. doi:10.1002/aja.1001180211

de Rooij, Dirk G. (2009). The spermatogonial stem cell niche. *Microscopy Research and Technique, 72*(8), 580-585. doi:10.1002/jemt.20699

DeFalco, T., Potter, S. J., Williams, A. V., Waller, B., Kan, M. J., & Capel, B. (2015). Macrophages contribute to the spermatogonial niche in the adult testis. *Cell Reports, 12*(7), 1107-1119. doi:10.1016/j.celrep.2015.07.015

Dietrich, D. R. (1993). Toxicological and pathological applications of proliferating cell nuclear antigen (PCNA), a novel endogenous marker for cell proliferation. *Critical Reviews in Toxicology, 23*(1), 77-109. doi:10.3109/10408449309104075

Dobson, S., & Dodd, J. M. (1977). Endocrine control of the testis in the dogfish *Scyliorhinus canicula* L. II. Histological and ultrastructural changes in the testis after partial hypophysectomy (ventral lobectomy). *General and Comparative Endocrinology, 32*(1), 53-71. doi:0016-6480(77)90082-X [pii]

Ema, H., & Suda, T. (2012). Two anatomically distinct niches regulate stem cell activity. *Blood, 120*(11), 2174-2181. doi:10.1182/blood-2012-04-424507

Foley, J. F., Dietrich, D. R., Swenberg, J. A., & Maronpot, R. R. (1991). Detection and evaluation of proliferating cell nuclear antigen (PCNA) in rat tissue by an improved immunohistochemical procedure. *The Journal of Histotechnology, 14*(4), 237-241. doi:10.1179/his.1991.14.4.237

Gautier, A., Bosseboeuf, A., Auvray, P., & Sourdaine, P. (2014). Maintenance of potential spermatogonial stem cells in vitro by GDNF treatment in a chondrichthyan model

(*Scyliorhinus canicula* L.). *Biology of Reproduction, 91*(4), 1-15. doi:10.1095/biolreprod.113.116020

Grier, Harry J. (1992). Chordate testis: The extracellular matrix hypothesis. *J Exp Zool, 261*(2), 151-160. doi:10.1002/jez.1402610206

Haczkiewicz, K., Rozenblut-Kościsty, B., & Ogielska, M. (2017). Prespermatogenesis and early spermatogenesis in frogs. *Zoology, 122*, 63-79. doi:https://doi.org/10.1016/j.zool.2017.01.003

Hall, P. A., & Woods, A. L. (1990). Immunohistochemical markers of cellular proliferation: achievements, problems and prospects. *Cell and Tissue Kinetics, 23*, 505-522.

Hilscher, B., Hilscher, W., & Maurer, W. (1966). [Autoradiographic determination of the generation time and division phases of different generations of spermatogonia in the rat]. *Naturwissenschaften, 53*(16), 415-416.

Huckins, C. (1971a). Cell cycle properties of differentiating spermatogonia in adult Sprague-Dawley rats. *Cell and Tissue Kinetics, 4*(2), 139-154.

Huckins, C. (1971b). The spermatogonial stem cell population in adult rats. *Cell Proliferation, 4*(4), 313-334. doi:10.1111/j.1365-2184.1971.tb01543.x

Hutchison, C., & Kill, I. (1989). Changes in the nuclear distribution of DNA polymerase alpha and PCNA/cyclin during the progress of the cell cycle, in a cell-free extract of *Xenopus* eggs. *Journal of Cell Science, 93*, 605-613.

Ishii, K., Kanatsu-Shinohara, M., & Shinohara, T. (2014). Cell-cycle-dependent colonization of mouse spermatogonial stem cells after transplantation into seminiferous tubules. *The Journal of Reproduction and Development, 60*(1), 37-46.

Kerr, J. B. (1995). Macro, micro, and molecular research on spermatogenesis: the quest to understand its control. *Microscopy Research and Technique, 32*(5), 364-384. doi:10.1002/jemt.1070320503

Loppion, G., Crespel, A., Martinez, A.-S., Auvray, P., & Sourdaine, P. (2008). Study of the potential spermatogonial stem cell compartment in dogfish testis, *Scyliorhinus canicula* L. *Cell and Tissue Research, 332*(3), 533-542.

McClusky, L. M. (2005). Stage and season effects on cell cycle and apoptotic activities of germ cells and Sertoli cells during spermatogenesis in the spiny dogfish (*Squalus acanthias*). *Reproduction, 129*(1), 89-102. doi:129/1/89 [pii]10.1530/rep.1.00177

McClusky, L. M. (2012). Coordination of spermatogenic processes in the testis: lessons from cystic spermatogenesis. *Cell Tissue Res, 349*(3), 703-715. doi:10.1007/s00441-011-1288-1

McClusky, L. M. (2013). The caspase-dependent apoptosis gradient in the testis of the blue shark, *Prionace glauca*. *Reproduction, 145*(3), 297-310.

McClusky, L. M. (2018). Multiple sources for Sertoli cells and two Sertoli phenotypes in the adult elasmobranch testis: Insight from two species belonging to different orders. *The Anatomical Record, 301*(11), 1944-1954. doi:10.1002/ar.23949

Meng, X., Lindahl, M., Hyvonen, M. E., Parvinen, M., de Rooij, D. G., Hess, M. W., . . . Sariola, H. (2000). Regulation of cell fate decision of undifferentiated spermatogonia by GDNF. *Science, 287*(5457), 1489-1493. doi:8297 [pii]

Miething, A. (2010). Local desynchronization of cellular development within mammalian male germ cell clones. *Annals of Anatomy, 192*(4), 247-250. doi:10.1016/j.aanat.2010.06.004

Nel-Themaat, L., Vadakkan, T. J., Wang, Y., Dickinson, M. E., Akiyama, H., & Behringer, R. R. (2009). Morphometric analysis of testis cord formation in Sox9-EGFP mice. *Developmental Dynamics, 238*(5), 1100-1110. doi:10.1002/dvdy.21954

Nóbrega, R. H., Greebe, C. D., van de Kant, H. J., Bogerd, J., de França, L. R., & Schulz, R. W. (2010). Spermatogonial Stem Cell Niche and Spermatogonial Stem Cell

Transplantation in Zebrafish. *PLoS One*, *5*(9), e12808. doi:10.1371/journal.pone.0012808

Oatley, J. M., & Brinster, R. L. (2012). The germline stem cell niche unit in mammalian testes. *Physiological Reviews, 92*(2), 577.

Panda, R. P., Barman, H. K., & Mohapatra, C. (2011). Isolation of enriched carp spermatogonial stem cells from Labeo rohita testis for in vitro propagation. *Theriogenology*, *76*(2), 241-251. doi:10.1016/j.theriogenology.2011.01.031

Parsons, G. R., & Grier, H. J. (1992). Seasonal changes in shark testicular structure and spermatogenesis. *Journal of Experimental Zoology*, *261*(2), 173-184.

Piferrer, F. C., & Callard, G. V. (1995). Inhibition of deoxyribonucleic acid synthesis during premeiotic stages of spermatogenesis by a factor from testis-associated lymphomyeloid tissue in the dogfish shark (*Squalus acanthias*). *Biology of Reproduction*, *53*(2), 390-398.

Plant, T. M. (2010). Undifferentiated primate spermatogonia and their endocrine control. *Trends in Endocrinology & Metabolism, 21*(8), 488-495. doi:https://doi.org/10.1016/j.tem.2010.03.001

Potter, S. J., & DeFalco, T. (2017). Role of the testis interstitial compartment in spermatogonial stem cell function. *Reproduction, 153*(4), R151-r162. doi:10.1530/rep-16-0588

Pratt, H. L. (1979). Reproduction in the blue shark, *Prionace glauca*. *Fishery Bulletin*, *77*(2), 445-470.

Pratt, H. L. (1988). Elasmobranch gonad structure: a description and survey. *Copeia*, *3*, 719-729.

Prelich, G., Tan, C.-K., Kostura, M., Mathews, M. B., So, A. G., Downey, K. M., & Stillman, B. (1987). Functional identity of proliferating cell nuclear antigen and a DNA polymerase-δ auxiliary protein. *Nature, 326*(6112), 517-520. doi:10.1038/326517a0

Prieur, D. J., Fenstermacher, J. D., & Guarino, A. M. (1976). A choroid plexus papilloma in an elasmobranch (*Squalus acanthias*). *Journal of the National Cancer Institute, 56*(6), 1207-1209.

Rastogi, R. K., DiMeglio, M., DiMatteo, L., Minucci, S., & Iela, L. (1985). Morphology and cell population kinetics of primary spermatogonia in the frog (*Rana esculenta*) (Amphibia: Anura). *Journal of Zoology, 207*(3), 319-330. doi:10.1111/j.1469-7998.1985.tb04934.x

Saunders, P. T. (2003). Germ cell-somatic cell interactions during spermatogenesis. *Reproduction Supplement, 61*, 91-101.

Schlatt, S., & Weinbauer, G. E. (1994). Immunohistochemical localization of proliferating cell nuclear antigen as a tool to study cell proliferation in rodent and primate testes. *International Journal of Andrology, 17*(4), 214-222. doi:10.1111/j.1365-2605.1994.tb01245.x

Simpson, T. H., & Wardle, C. S. (1967). A seasonal cycle in the testis of the spurdog, *Squalus acanthias*, and the sites of 3β-hydroxysteroid dehydrogenase activity. *Journal of the Marine Biological Association of the United Kingdom, 47*, 699-708.

Skinner, M. K. (1990). Mesenchymal (stromal)-epithelial cell interactions in the testis and ovary which regulate gonadal function. *Reproduction, Fertility and Development, 2*(3), 237-243. doi:https://doi.org/10.1071/RD9900237

Smith, J. F., Yango, P., Altman, E., Choudhry, S., Poelzl, A., Zamah, A. M., . . . Tran, N. D. (2014). Testicular niche required for human spermatogonial stem cell expansion. *Stem Cells Translational Medicine, 3*(9), 1043-1054. doi:10.5966/sctm.2014-0045

Wrobel, K. H., Bickel, D., & Kujat, R. (1996). Immunohistochemical study of seminiferous epithelium in adult bovine testis using monoclonal antibodies against Ki-67 protein and proliferating cell nuclear antigen (PCNA). *Cell and Tissue Research, 283*(2), 191-201.

Yazawa, T., Yamamoto, T., Nakayama, Y., Hamada, S., & Abé, S. (2000). Conversion from mitosis to meiosis: Morphology and expression of proliferating cell nuclear antigen (PCNA) and Dmc1 during newt spermatogenesis. *Development, Growth & Differentiation, 42*(6), 603-611. doi:10.1046/j.1440-169x.2000.00544.x

Yoshida, S., Sukeno, M., & Nabeshima, Y. (2007). A vasculature-associated niche for undifferentiated spermatogonia in the mouse testis. *Science, 317*(5845), 1722-1726. doi:1144885 [pii]10.1126/science.1144885

FIGURE LEGENDS

Figure 1. The tissue architecture of the immature pole of the testis of *P. glauca* (A) illustrated schematically and (B) following PCNA immunohistochemical staining of paraffin cross-sections. (A) A fibrous germinal ridge (GR) delimits the outer boundary of the immature pole. Distally to the GR is the germinal zone (GZ) where spermatocysts are assembled. The latter first appear as non-patterned and then patterned, based on the arrangement, or lack of it, of the nuclei of the Sertoli cells and spermatogonia relative to each other. (B) The exquisite PCNA immunolabeling of the spermatogonia delineates the outer boundaries of the germinal nests (circled areas) in the otherwise dense GR stroma (st). PCNA immunohistochemistry greatly facilitates the immunodetection of the A-spermatogonia wherever they may be found, freed from a nest (black filled arrow), or at the GR – GZ transition. Large stromal cells (black-white arrow) that surround single A-spermatogonia ultimately become arranged in rows adjacent to

the latter. *Inset*: High power view of two nest-located A-spermatogonia with their voluminous cytoplasm and speckled nuclei are tightly flanked by a fusiform somatic cell (open arrows). Spermatogonium's cell membrane (arrowheads). Bar = 30 µm.

Figure 2. Heterogeneity of type A spermatogonia in the GR as per their PCNA immunoreactivities. (A) Type A spermatogonia can be grouped into those with PCNA-negative speckled (*neg*), light and dark speckled brown (*lsp*, *dsp*) and intense homogeneous dark brown (*hod*) nuclei, the latter usually revealing a single blue-grey nucleolus (nu). (B, C) Another constituent element of the GR, namely large oblong cells (circled area, black filled arrows) may aggregate around scatterings of single and small clusters of A-spermatogonia (asterisks), or typically among dispersed-looking A^{hod}-spermatogonia that noticeably lack associated fusiform cells (open arrows). *Insets*: Loss of PCNA immunoreactivity in A^{hod}-spermatogonia is dramatic and systematic. (D) On rare occasions, A^{hod}-spermatogonia are observed as part of a chain of other immunonegative cells with ovoid nuclei (arrowheads). Shared features such as the prominent nucleolus and the remnants of PCNA immunoreactivity (white arrowheads) suggest an affiliation between these cells. *Inset*: Differences between the A-spermatogonia as revealed by H&E staining. (E, F) For purposes of comparison, rarely seen dying A-spermatogonia (blue asterisk) may appear shrunken and intensely brown in color, or as a blue mass of compacted chromatin surrounded by immunostained cell debris. Fusiform somatic cell (open arrows). Bars: (A, C, D, E, F) = 10 µm, B = 20 µm

Figure 3. Percentages of the three types of PCNA-immunoreactivity among A-spermatogonia expressed as a function of the spermatogonium's closest aligned somatic cell type in the GR of *P. glauca*. Spermatogonia with immunonegative speckled nuclei, though very rarely

observed, were grouped together with the A^{lsp}-spermatogonia. For the sake of simplicity, the counts of the A^{hod}- spermatogonia included both partially (blue-brownish) immunostained and blue-stained spermatogonia. Values represent the untransformed mean percentage ± S.E.M of type A-spermatogonia analyzed by one-way ANOVA. The Student Newman-Keuls multiple-comparison test was used to determine mean differences between the proportions of the three types of PCNA-immunostained A-spermatogonia associated with their respective somatic cell type. Different letters indicate statistically significant differences ($P<0.001$). Numbers in parentheses along the x-axis indicate the respective numbers of A-spermatogonia counted in each category.

Figure 4. Overview of a GZ histoarchitecture showing a germ line that consists nearly exclusively of homogeneous dark brown and related spermatogonia. (A) Differential PCNA immunostaining in a group of A^{hod}- progenitors (black open arrows). Some display a markedly diffuse immunostaining pattern (green asterisks) while another is already in mitosis (red asterisk). (B) The further rearrangement of the somatic (black filled arrows, blue underlined) and germ cells (all open arrows) are concomitant with intricate changes in the latter, including the unveiling of globular translucent areas (double-headed arrows) that eventually fill the entire nucleus (red arrow). The latter are coincident with the assembly of the first cysts with the distinct lumena (L) and oblong stromal cell-derived Sertoli cells (black underlined). (C) An array of related increasingly diffuse immunostaining patterns (red arrows, black double-headed open arrows, green asterisks) can be observed in growing, mitotically active cyst stages during which the Sertoli cell nuclei (black filled arrowheads) begin to assume a perilumenar position (nuclei abutting black rings). (D) Early B^{hod}- spermatogonia in nonpatterned cysts may alternatively display diminishing PCNA immunoreactivity with

resultant basophilia (black open arrows). Such cysts are devoid of mitotic figures. Bars: (A, B, C) = 10 µm, D = 20 µm

Figure 5. Overview of a GZ histoarchitecture showing a germ line that display nearly exclusively dark speckled brown immunostaining. The appearance of assemblages (blue circled) of stromal cells (filled arrows) and committed A- progenitors and/or their progeny (black and red asterisks) presage the imminent assembly of the first cysts (black circled) with similar-looking early B-spermatogonia (black asterisks). *Inset*: The expansion, in such GZs, of the *dsp* immunomorphology outstrips that of the germ line that displays the *hod* immunomorphology. Sertoli cells (filled arrowheads); st, stroma. Bar = 10 µm.

Figure 6. The changing immunoreactivities of B^{hod} -spermatogonia in early patterned cysts. The presence of uneven light brown, globular-like spermatogonia (green asterisks) adjacent to B^{hod}-spermatogonia in the peripheral layer of spermatogonia (black brackets) is due to the increased appearance *of globular-like lighter colored areas* (open arrowheads) in the latter. These developments also account for numerous such cysts (boxed green asterisks). *Insets*: *(left)* The broad designation as the uneven light brown, globular-like appearance (green asterisks) includes other successive intricate changes in the spermatogonia, including the display of tortuous blue profiles against a beige background (green asterisk^{1}), a state with increasing separation of chromatin into distinct punctate blue (green asterisk^{2}), and further overt thickening of the blue chromatin strands (green asterisk^{3}). The latter two changes are the clearest indication of prophase (P). *(right)* This anomalously immunostained

spermatogonium with condensed chromatin (blue asterisk) indicates a dying spermatogonium. For purposes of comparison, the PCNA-negative condensed chromatin of a dividing Sertoli cell in anaphase (double red asterisk). Perilumenar Sertoli cell nuclei (blue brackets; filled arrowheads). Bar= 20 µm,

Figure 7. Frequency of mitotic figures per cyst (non-patterned and earliest patterned) housing either unevenly light brown/globular appearing or homogeneously dark brown stained and related B-spermatogonia, expressed as a function of testicular condition (n=11). Values represent the averages of square root transformed counts of mitotic figures ± SEM per cyst that intersected four lines analyzed by one-way ANOVA. The Student Newman-Keuls multiple comparison test was used to identify mean percentages that differed significantly. Different letters (a, c; $P<0.01$; x, y; $P<0.05$) and asterisks ($P<0.001$) indicate significant differences. MNC, multinucleate cell death, Vac, vacuolated condition.

Figure 8. Changes in the architectural pattern of PCNA immunostaining in early B-spermatogonia in nonpatterned cysts expressed as a function of testicular condition in summer-caught *P. glauca* specimens (n=10). Values represent the mean percentage ± S.E.M of non-patterned cysts whose spermatogonia display a given type of PCNA immunostaining architecture analyzed by one-way ANOVA. The Student Newman-Keuls multiple comparison test was used to identify mean percentages that differed significantly. Different letters (a and c, $P<0.001$) and asterisks (single, $P<0.05$; double, $P<0.01$) indicate significant differences.

Figure 9. A tentative scheme for putative functional interrelationships between the stem cell region (GR) and the premeiotic region of the testis of *P. glauca* (actual cell lineages not

implied). Basophilic GR-located A^{hod}-spermatogonia ($A^{hod(neg)}$) and identical committed A^{hod}-progenitors ($A^{hod\ (neg)}$) in the GZ most likely represent those that exited the cell cycle. The ensuing appearance of spermatogonial cysts with one, two or more peripheral layers of spermatogonia (a, c) whose immunomorphologies strongly resemble the immunomorphologies of their respective committed A-progenitors upstream in the GZ suggest differing rates of cycling through G2-phase (a), and G1– S-phase (c). G2-phase B^{hod}-spermatogonia in some cysts may be protracted/delayed (b) as evident from the presence of multiple rows of such cysts in some testes. See *Discussion*. A^{res}, putative A-reserve spermatogonial stem cells.

Figure 1.

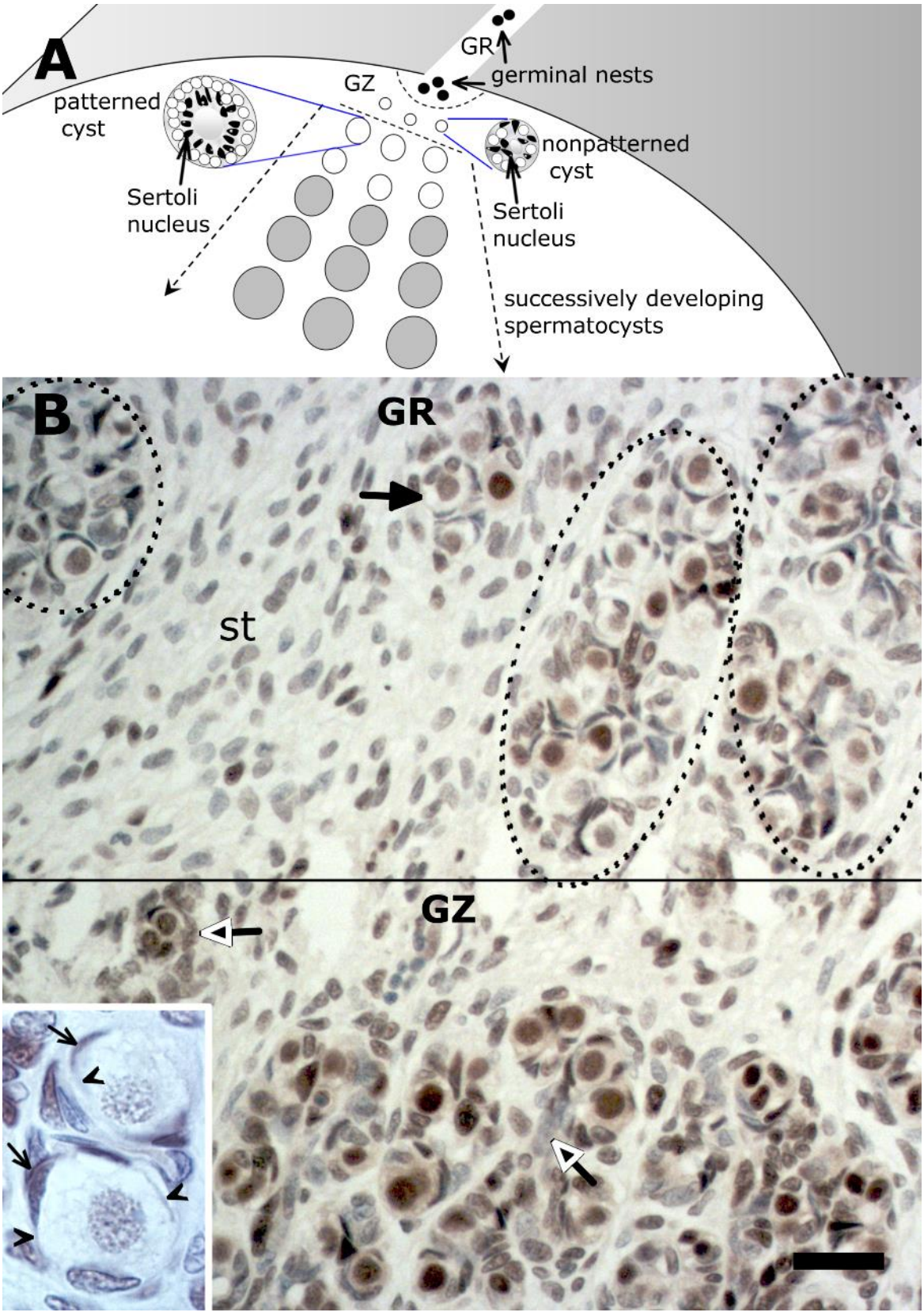
A
GR
germinal nests
GZ
patterned
cyst
nonpatterned
cyst
Sertoli
nucleus
Sertoli
nucleus
successively developing
spermatocysts
B
GR
st
GZ

Figure 2.

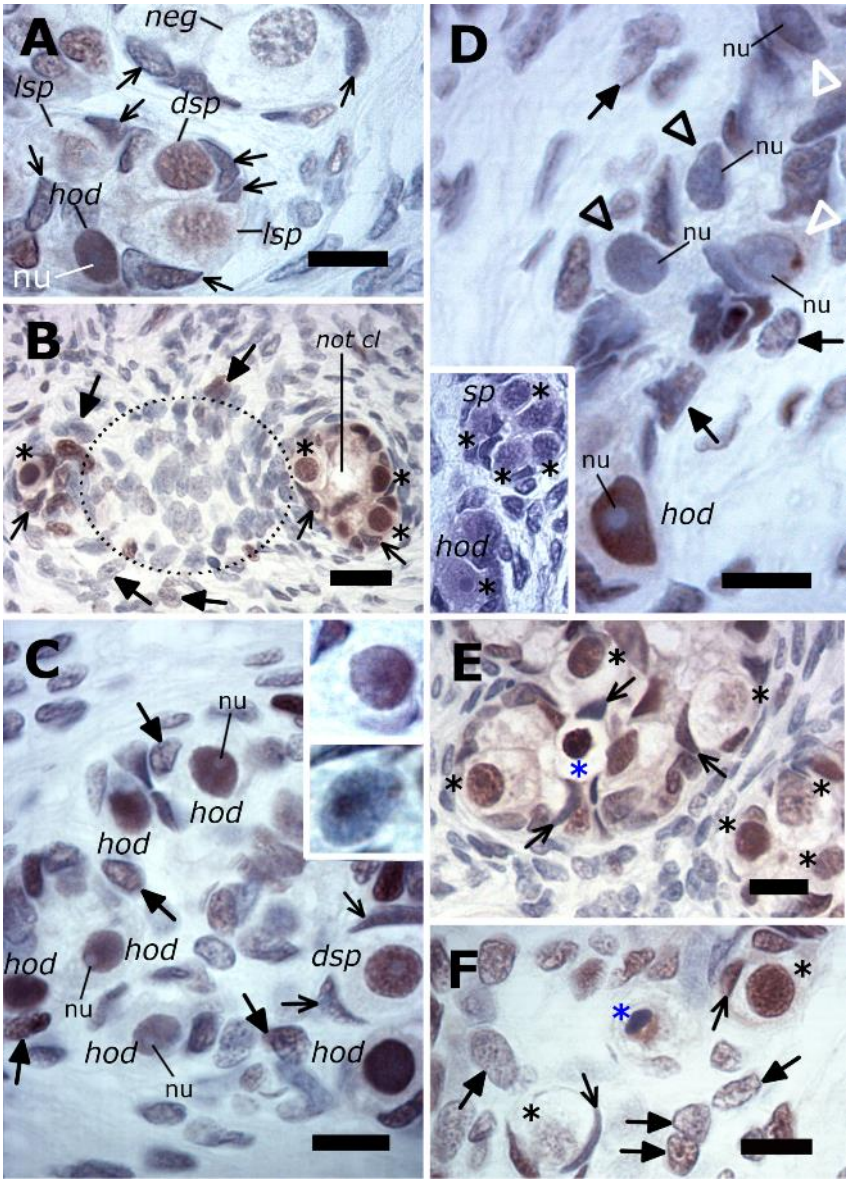
A
neg
lsp
dsp
hod
lsp
nu
B
not cl
C
nu
hod
hod
hod
hod
dsp
nu
hod
nu
hod
D
nu
nu
nu
nu
sp
hod
nu
hod
E
F

Figure 3.

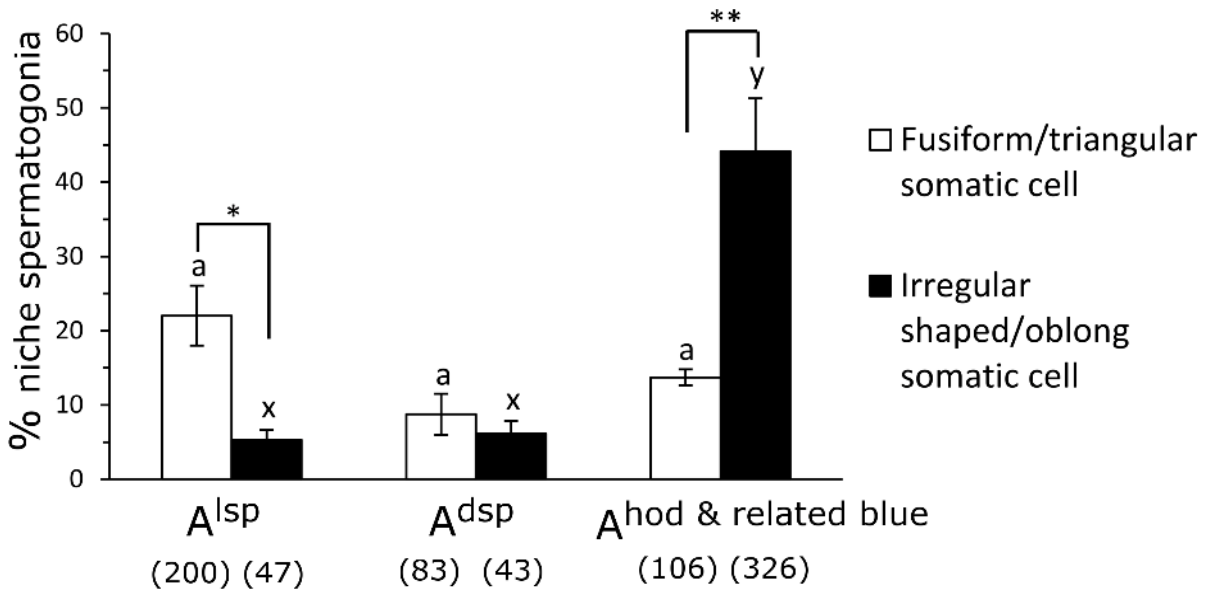
% niche spermatogonia
60
50
40
30
20
10
0
*
**
a
x
a
x
a
y
Fusiform/triangular somatic cell
Irregular shaped/oblong somatic cell
A lsp
(200) (47)
A dsp
(83) (43)
A hod & related blue
(106) (326)

Figure 4.

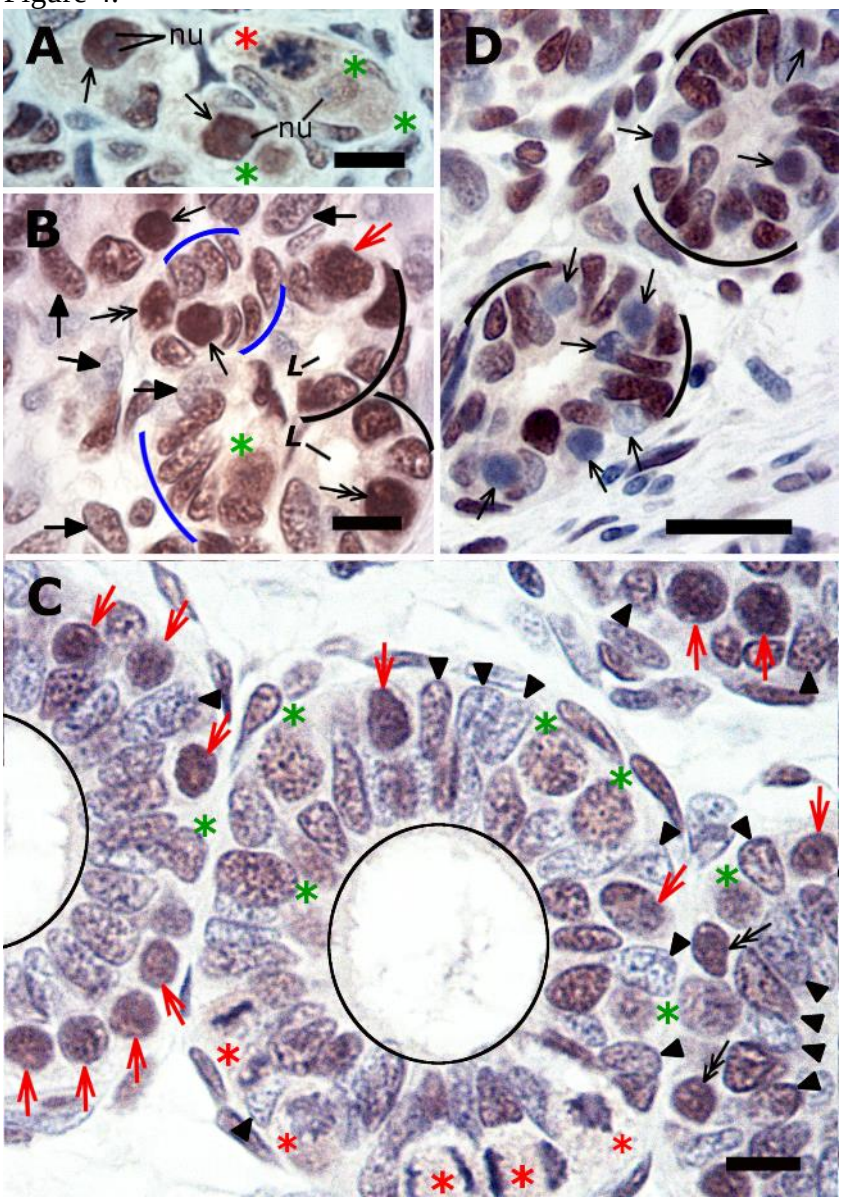

Figure 5.

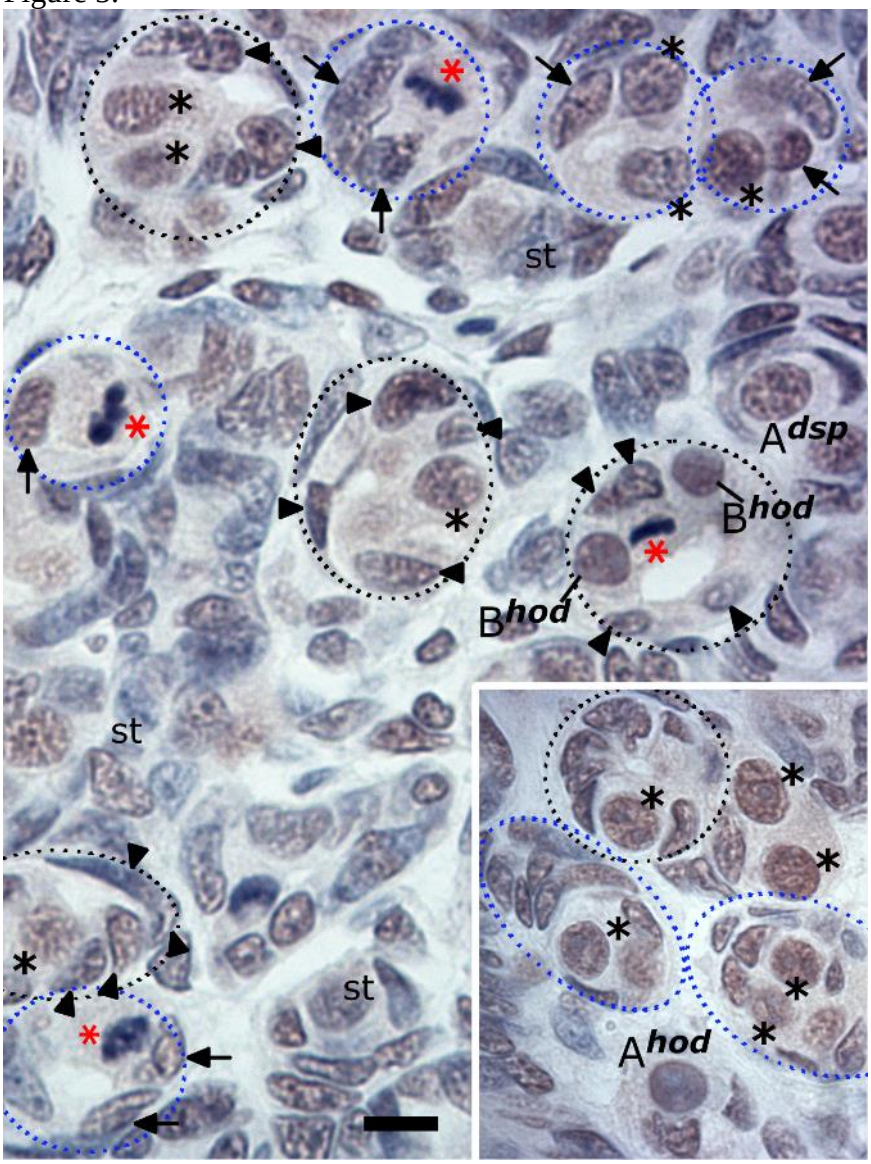

Figure 6.

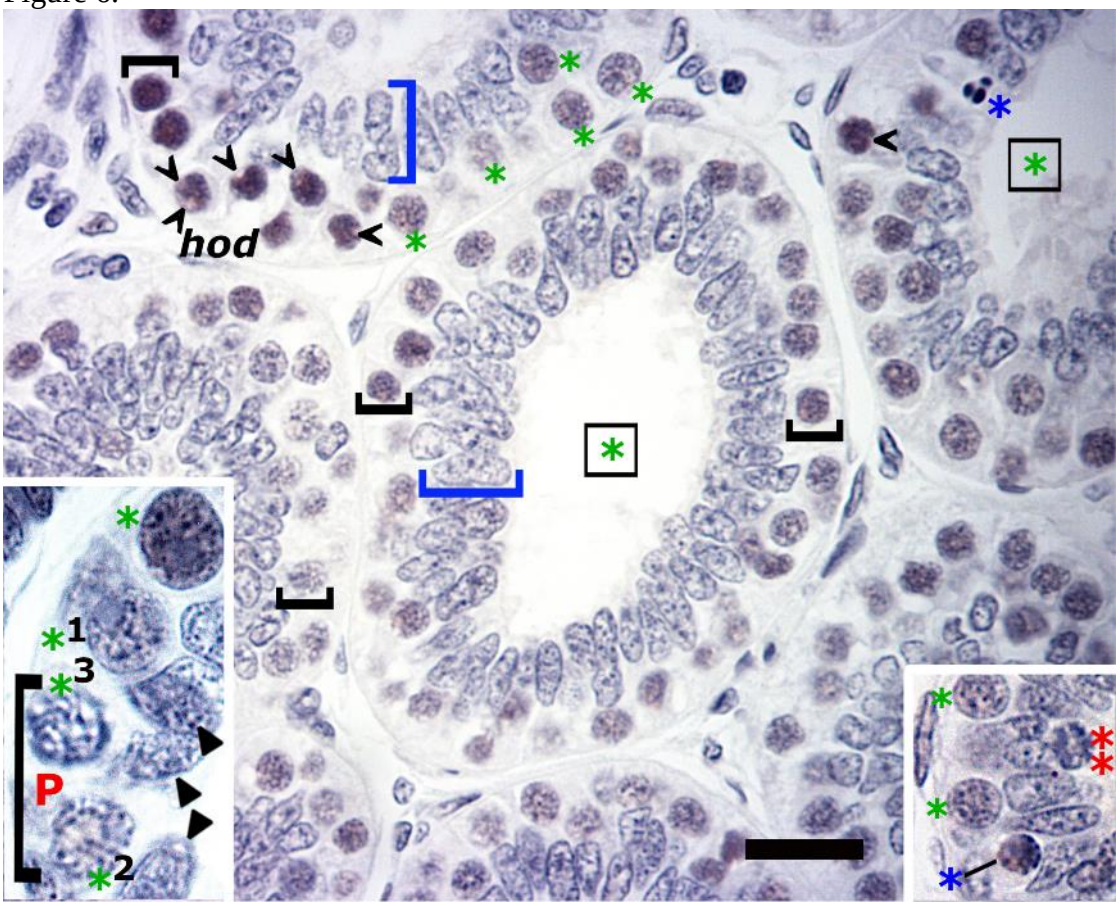

Figure 7.

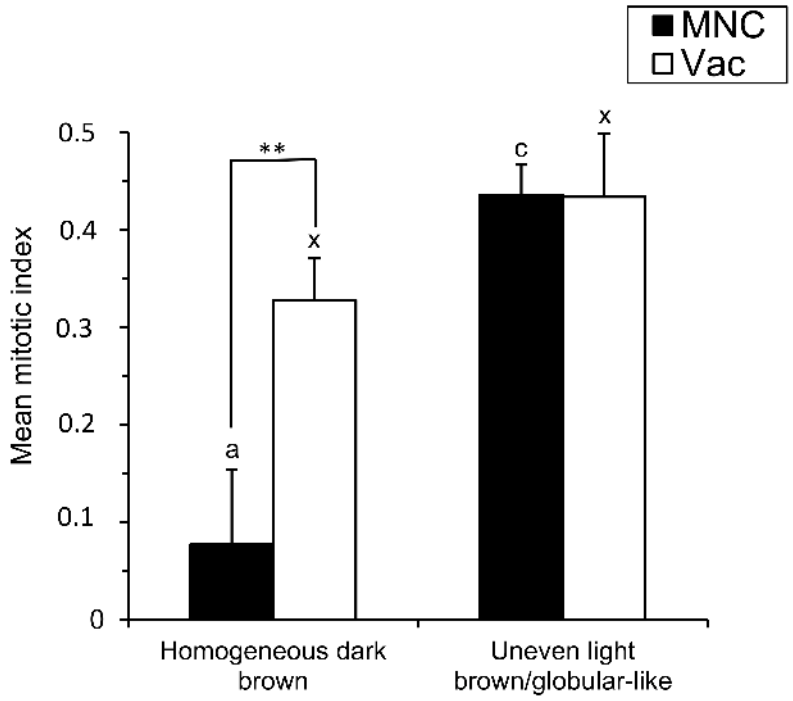

Figure 8.

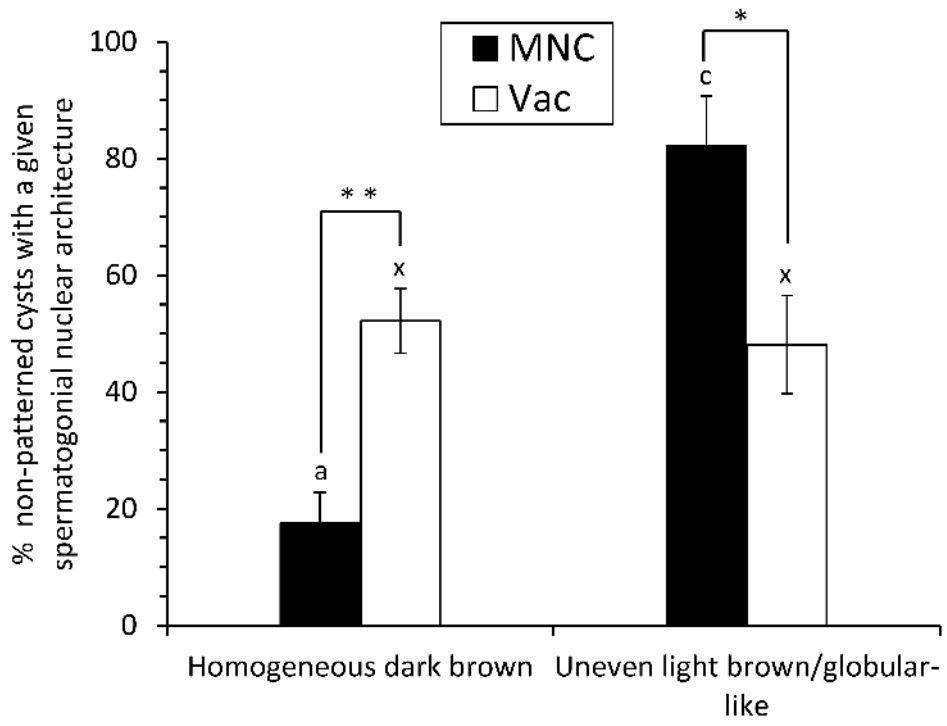
MNC
Vac
% non-patterned cysts with a given spermatogonial nuclear architecture
100
80
60
40
20
0
* *
*
a
x
c
x
Homogeneous dark brown
Uneven light brown/globular-like

Figure. 9.

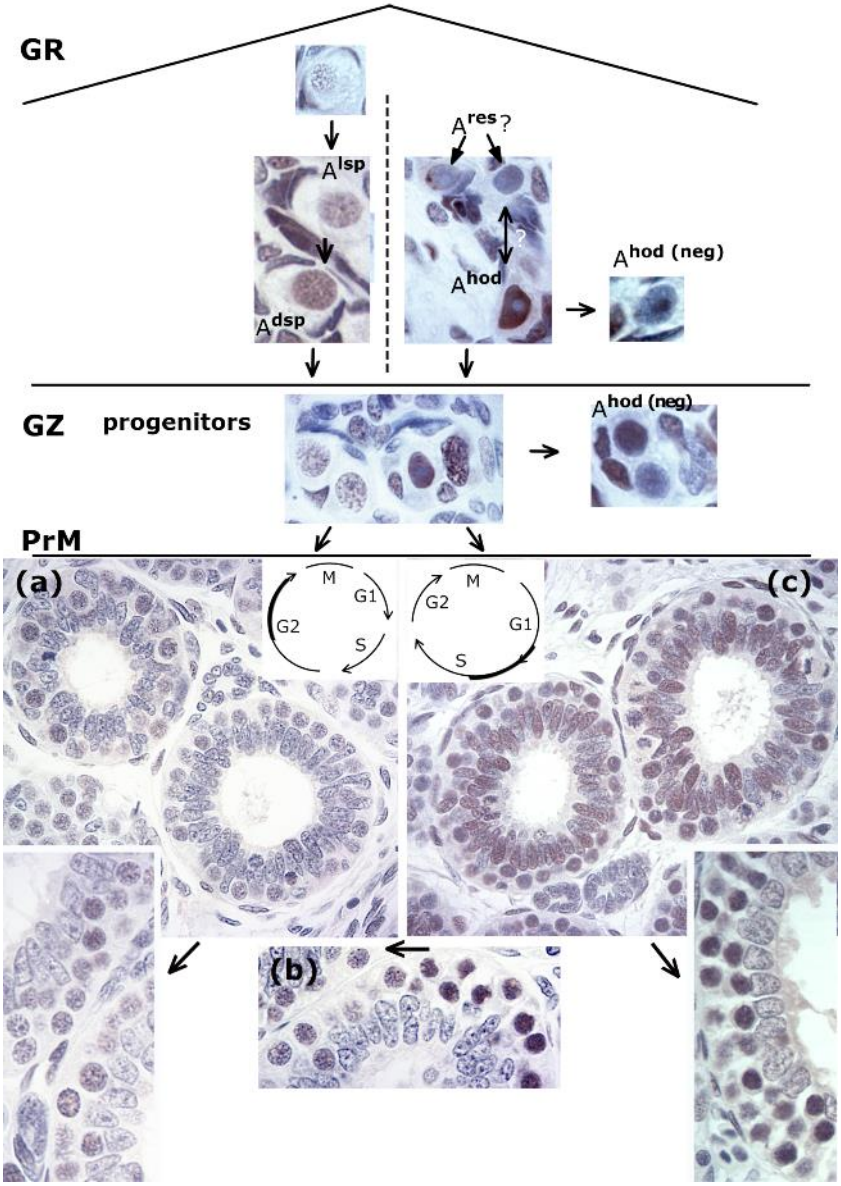
GR
A res ?
A lsp
A dsp
A hod
?
A hod (neg)
GZ progenitors
A hod (neg)
PrM
(a)
M
G1
G2
S
M
G2
G1
S
(c)
(b)